Available online at www.sciencedirect.com
SCIENCE DIRECT®
International Journal of Mass Spectrometry 233 (2004) 181–192
International Journal of Mass Spectrometry
www.elsevier.com/locate/ijms

High resolution study of cluster anion formation in low-energy electron collisions with OCS clusters

S. Barsotti [a], T. Sommerfeld [b], M.-W. Ruf [a], H. Hotop [a,*]

[a] *Fachbereich Physik, Universität Kaiserslautern, D-67653 Kaiserslautern, Germany*
[b] *Theoretische Chemie, Universität Heidelberg, D-69120 Heidelberg, Germany*

Received 30 September 2003; accepted 21 December 2003

Abstract

Using the laser photoelectron attachment (LPA) method involving a supersonic target beam with carbonyl sulfide molecules (OCS) seeded in helium, we have studied the formation of cluster anions in low-energy electron attachment (E = 1–200 meV) to molecular clusters of OCS at high resolution (energy width 1–2 meV). Homogeneous cluster anions $(OCS)_q^-$ (q = 1–12) are predominantly formed. In addition, due to CS_2 impurities in the OCS sample, mixed cluster anions ($(OCS)_{q-1}CS_2^-$, $q \geq 1$) are observed at levels of a few percent. The energy dependences of cluster anion formation are characterized by a strong rise towards zero energy attributed to s-wave attachment as well as—below the onsets of the (0 1 0), (0 0 1), and (0 2 0) vibrational modes of the OCS molecule—by vibrational Feshbach resonances (VFR) whose importance decreases towards larger cluster sizes q. Formation of the $(OCS)_2^-$ anion is especially enhanced at near-zero electron energies; moreover, the attachment spectrum exhibits a sharp VFR resonance just below the onset for excitation of the (0 2 0) mode in the OCS molecule. The electron attachment behaviour of OCS clusters is intermediate between that of CO_2 clusters (which is dominated by VFRs) and that of CS_2 (which exhibits a strong zero energy peak, but no VFRs). This finding is correlated with the properties of the respective molecular neutrals and anions which have been studied using high level ab initio methods. We also report the energetics of the neutral and the anion dimer species. The role of VFRs as doorway states into valence-type anion states is discussed.

PACS: 34.80.Ht; 36.40.Wa; 34.80.Gs; 36.40.Qv

Keywords: Electron attachment; OCS clusters; Cluster anions

1. Introduction

Temporary negative ion states XY^{-*} are known to be crucial for vibrational excitation [1–6] and negative ion formation [1–4,6–8] in low energy collisions of electrons with molecules XY and clusters $(XY)_N$ ($N \geq 2$) (described by a set of quantum numbers $\{\alpha\}$ denoting its electronic and ro-vibrational state):

$$(XY)_N\{\alpha\} + e^-(E) \rightarrow (XN)_N{}^{-*} \rightarrow (XY)_N\{\alpha'\} + e^-(E') \quad (1a)$$

$$\rightarrow (XY)_{q-1}Y^- + X + (N-q)XY, \quad (q \leq N) \quad (1b)$$

$$\rightarrow (XY)_q{}^- + (N-q)XY, \quad (q < N) \quad (1c)$$

$$\rightarrow (XY)_N{}^{-\ddagger} \quad (\tau > 100\,\mu s) \quad (1d)$$

Here path (1a) describes elastic ($\alpha = \alpha'$) or inelastic scattering. Process (1b) represents dissociative electron attachment (DA) while in the reaction (1c) (only relevant for clusters, i.e., $N \geq 2$) anion formation proceeds through evaporation of XY constituents. Even if no other stabilizing process occurs, the temporary negative ion $(XY)_N{}^{-*}$ ($N \geq 1$) can become metastable with respect to spontaneous re-emission (autodetachment) of the electron, if the electronic energy is rapidly redistributed into internal degrees

* Corresponding author.

1387-3806/$ – see front matter © 2004 Elsevier B.V. All rights reserved.
doi:10.1016/j.ijms.2003.12.015

of freedom (intra- and intermolecular vibration, rotation), thereby yielding long-lived negative ions $(XY)_N^{-\ddagger}$ in path (1d), e.g., $SF_6^{-\ddagger}$ from SF_6 [6,9–11] or small $(H_2O)_N^{-\ddagger}$ anions ($N = 2$, 6, 7) [12]. Let us emphasize at this point that targets of molecular clusters $(XY)_N$, typically created in supersonic beams, contain a broad distribution of sizes N. As a consequence, the correlation of the observed anion cluster size q with the size N of the neutral cluster precursor relevant for the reactions (1) is thus not a priori known.

One of the interesting features of clusters is their role as nanoscale prototypes for studying the effects of solvation on the characteristics of both solvent and solvated particle, due to the interaction between a solvated molecule or ion and its surrounding solvent environment. Solvation effects also play a key role in the formation of negative ions by attachment of slow electrons to molecular clusters. The anion resonances, observed for single molecules, appear shifted towards lower energies in clusters due to the effects of solvation [7,8]. For molecular clusters additional features may be observed which reflect the effects of the cluster environment on the resonance energy and symmetry. One aspect is the appearance of anion resonances in clusters whose formation is symmetry-forbidden for the isolated molecule [7,13]. Another intriguing result in early studies of cluster anion formation was the observation of a prominent resonance at zero energy in cases where such a feature is absent in the monomer [7,14] (e.g., for clusters of CO_2 [15–17], N_2O [15,16], and H_2O [18]), but the true nature of this "zero energy resonance" remained uncertain for some time.

Using the laser photoelectron attachment (LPA) method at energy widths around 1 meV, our group has recently demonstrated that the cluster anion yield in electron collisions with clusters of $XY = N_2O$ [19,20] and CO_2 [21,22] over the energy range 0–200 meV is to a large extent mediated by narrow vibrational Feshbach resonances (VFRs) [6,23], i.e., temporary negative ion states of the type $[(XY)_{N-1}XY(\nu_i \geq 1)]^-$ which occur at energies below those of the neutral cluster $[(XY)_{N-1}XY(\nu_i \geq 1)]$ (here the vibrational excitation ν_i in the VFR and the neutral cluster is meant to be the same). It was thus shown for N_2O [19,20] and CO_2 clusters [21,22] that the broad "zero energy resonance," as observed in the early work at energy widths around 0.5 eV [7,14,16,17], is due to the combined influence of the previously non-resolved, overlapping VFRs and (notably for N_2O clusters) a sharp s-wave type enhancement of the cross section towards zero energy. For $XY = N_2O$, the VFRs were found to be extremely sharp with widths between 2 and 5 meV, to exhibit redshifts of less than 1 meV per added molecular unit, and to yield predominantly heterogeneous cluster anions $(N_2O)_{q-1}O^-$ ($q \geq 5$) [19,20], but also homogeneous cluster anions $(N_2O)_q^-$ ($q \geq 4$) [20]. Similar findings were reported for CO_2 clusters [21,22]. In that case, reaction (1b) does not contribute in a measurable extent to cluster anion formation at low electron energies, i.e., only homogeneous $(CO_2)_q^-$ anions ($q \geq 4$) were observed as decay products of the resonances. The VFRs are significantly broader than those for N_2O clusters (but still narrow, 10–20 meV) and exhibit larger red-shifts of about 12 meV per added monomer unit [21,22]. These findings show in a direct way that only few neutral precursor cluster sizes N (mainly one or two) lead to a certain anion size q. A simple model for the electron binding in the VFRs, involving the long-range electron-cluster polarization interaction and an essentially constant short range potential was able to reproduce the size-dependent redshift of the VFRs [21,22] and indicated that the size q of the observed cluster anions does not differ much from the size N of the neutral cluster involved in the VFRs which decay to the observed anion (most likely $N - q = 0$ or 1).

Subsequent work on the formation of $(CS_2)_q^-$ ($q \geq 1$) cluster anions due to electron attachment to carbon sulfide clusters [22] yielded—in strong contrast to the situation for carbon dioxide clusters—smooth cross sections without VFR structure, showing s-wave behaviour near-zero energy and a monotonical decrease towards larger energies. This different behaviour was tentatively associated with the difference between the respective molecular electron affinities [22]. The observation of VFRs requires the existence of weakly-bound diffuse electron states, residing at the surface of the molecule or cluster and corresponding to long-range binding of the electron, e.g., due to dipolar or polarization forces [6,20–23]. In CO_2 electron scattering at low energies is dominated by a virtual state [6,24–26] which evolves into a weakly-bound state for clusters with sizes above about 4 [27]. Correspondingly, VFRs may be observed in anion yields for $q \geq 4$. For CS_2 the vertical electron affinity is near 0 eV [28], and one expects positive vertical electron affinities in CS_2 clusters due to the solvation shift; the anions should pick up progressively valence-type character, and this precludes the presence of VFRs. An example where solvation effects lead to disappearance of a VFR is the case of methyl iodide. A clear and prominent VFR has been observed for the CH_3I molecule just below the $\nu_3 = 1$ vibrational onset [23] while in the yield for $(CH_3I)_qI^-$ ($q = 1$, 2) cluster anion formation little ($q = 1$) and essentially no VFR structure ($q = 2$) is left [29].

In view of the strong differences between the attachment spectra for CO_2 and CS_2 clusters it is of obvious interest to investigate the attachment behaviour of OCS clusters with the aim to elucidate the evolution of VFR structure along the sequence CO_2, OCS, and CS_2. To our knowledge, the only previous work on energy-controlled cluster anion formation involving OCS clusters was carried out by Kondow and Mitsuke [30] who used Rydberg electron transfer (RET) to OCS clusters in a seeded supersonic beam from an ensemble of electron-excited Kr*(nl) Rydberg atoms with a band of principal quantum numbers around $n \approx 25$. Under their experimental conditions, the anion mass spectrum was dominated by homogeneous $(OCS)_q^-$ anions with a maximum at the cluster size $q = 10$ [30]. We note that anion formation in dissociative electron attachment to OCS monomers at low energies is dominated by S^- formation, showing a

prominent peak at about 1.4 eV with a cross section of about 2.6×10^{-21} m^2 [31,32].

In the present work, we report the results of a high resolution study of the energy dependent yield for cluster anion formation due to low-energy attachment of free electrons (E = 1–200 meV) to molecular clusters in a supersonic beam of OCS molecules, seeded in helium carrier gas. Attachment spectra are presented for $(OCS)_q^-$ (q = 1–12) anions and also for the heterogeneous cluster anion species $(OCS)_qCS_2^-$ (q = 0, 1), formed in electron attachment to mixed $(OCS)_NCS_2$ clusters ($q \leq N$) present in the neutral cluster sample due to a CS_2 impurity. We also compare the evolution of the attachment spectra for formation of homogeneous cluster anions along the molecular series CO_2, OCS, and CS_2: while the CO_2 spectra are dominated by VFR structure, OCS presents an intermediate case, and for CS_2 no VFR structure is left in the spectra. The article is organized as follows. In Section 2 we discuss electron binding properties of OCS and its isovalent partners CO_2 and CS_2 and present some results of ab initio calculations regarding the respective potential energy surfaces; in Section 3, we dwell on the properties of the OCS dimer anion. In Section 4 we briefly address the experimental procedure and discuss some mass spectrometric test measurements. In Section 5 we present and discuss the experimental attachment spectra for homogeneous $(OCS)_q^-$ cluster anions and for some mixed cluster anions of the type $(OCS)_qCS_2^-$; we also compare the spectra observed for CO_2, OCS and CS_2 clusters and discuss the evolution along the molecular series. We conclude with a brief summary and some perspectives.

2. Electron binding properties of the CO_2, OCS, and CS_2 monomers

In this section we consider long-lived anionic states of the OCS monomer and its two isovalent partners CO_2 and CS_2. All three neutral molecules are linear in their closed-shell electronic ground states, and their structural properties are well documented in the literature (e.g., [33]). For convenience in the discussions below, we note that the lowest vibrationally excited states of OCS, labeled (ν_1 ν_2 ν_3), are the bending mode (0 1 0) (64.5 meV), the CS stretch mode (0 0 1) (106.5 meV) and the bending overtone (0 2 0) (129.0 meV). The CO stretch mode (1 0 0) (255.7 meV) [34] is energetically not accessible in the energy range of the present experiment.

In contrast, the properties of the associated anions, including the electron affinities, are still matter of debate. Most structural information on the anions stems from high level ab initio calculations, and an account of early work as well as reliable results for all three species can be found in [28]. Yet, in particular for the adiabatic electron affinity (AEA) of OCS (and CS_2) there is considerable disagreement between different computed values and values inferred from different experiments. For example, Compton et al. [35] deduced a value of AEA(OCS) = (0.46 ± 0.2) eV from charge transfer measurements involving alkali atoms with variable kinetic energy while Chen and Wentworth [36] deduced the lower limit AEA(OCS) ≥ 0.4 eV by using an electron capture detector operated in the pulse sampling mode at steady state. In contrast, Gutsev et al. [28] report a calculated value of AEA(OCS) = −0.22 eV, and most recently Surber et al. [37] conclude from their calculations that the AEA(OCS) is "either slightly negative or essentially zero."

Table 1
Adiabatic electron affinity (AEA) and vertical detachment energy (VDE) of CO_2, OCS, and CS_2

	AEA		ZPC	VDE	
	AUG3	AUG4	AUG3	AUG3	AUG4
CO_2	−635	−632	88	982	1028
OCS	−79	−77	70	1392	1437
CS_2	+376	+404	53	1320	1386

The values have been computed at the CCSD(T) level and do not include zero-point energies. Harmonic zero-point energy corrections (ZPC) for the AEA are given separately. All values in meV. Computed bond lengths R [10^{-10} m] and bond angles θ [°] obtained at the CCSD(T)/AUG3 level: CO_2: R_0(CO) = 1.1670; CO_2^-: R_-(CO) = 1.2368, θ_- = 137.6. OCS: R_0(CO) = 1.1625, R_0(CS) = 1.5747; OCS^-: R_-(CO) = 1.2130, R_-(CS) = 1.7162, θ_- = 136.2. CS_2: R_0(CS) = 1.5654; CS_2^-: R_-(CS) = 1.6462, θ_- = 142.7.
Note that the neutral molecules are linear (θ_0 = 180).

Here we present on the one hand very high level ab initio results for the AEA of all three isovalent molecules CO_2, OCS, and CS_2, and, on the other hand, cuts through the three respective potential energy surfaces (PES) that connect the equilibrium geometries of the neutral and the corresponding anionic species.

To compute the AEA as well as the vertical detachment energy (VDE) of the three systems the geometries (see Table 1) and the harmonic vibrational frequencies have been computed at the coupled cluster with single and double excitations and non-iterative triples (CCSD(T)) level, employing the augmented correlation-consistent triple-zeta (AUG3) basis set [38,39]. Single point energies at these geometries were then calculated at the CCSD(T) level, using the corresponding quadruple-zeta (AUG4) basis set [38,39], i.e., a [6s5p4d3f2g] set for carbon and oxygen and a [7s6p4d3f2g] set for sulfur. (Note that in the next section the associated double-zeta (AUG2) basis set is used in addition.) Whereas the calculations of the AEA involve only anionic states that are clearly stable with respect to vertical detachment, the cuts through the PES contain regions where the detachment energy becomes very small and the bound anionic states are transferred into resonances. In these regions very diffuse basis functions are needed, and the description of the anionic states based on a single unrestricted Hartree–Fock (HF) or restricted HF reference function can break down [27,40]. Thus, to compute the cuts through the PES the equation-of-motion coupled-cluster (EOM-CCSD) method [41] was employed and the AUG3 basis set was

further augmented with a [4s4p2d] set of diffuse functions (even scaled exponents starting from the smallest respective exponents in the AUG3 sets, scaling factor $10^{1/2}$). In all calculations the core electrons were frozen in their HF orbitals. The calculations were performed using the ACES II computer code [42].

The results for the AEA and VDE are collected in Table 1. Taking the uncorrected AUG4 values and the harmonic zero-point correction we arrive at AEA values of −544 meV for CO_2, −7 meV for OCS, and +457 meV for CS_2. These values are consistently more positive than the most reliable results from reference [28], and our AEA for OCS of essentially 0 eV is in line with the conclusions reached in [37].

We are confident that the values are well converged from a one-particle basis set point of view, since the computed values change only very little in going from the AUG3 to the AUG4 basis set, but there may of course be small shifts due to correlation effects beyond CCSD(T) and due to the correlation of the core electrons. Based on the comparison with analogous calculations for the well known EA of the O and S atoms, we conclude that the errors of our results should be at most in the order of 50 meV. Thus, the findings put a question mark on several of the experimental values and call for a reexamination of the data.

Whereas the individual AEA and VDE values are certainly important by themselves, a more complete picture of the electron binding properties can be obtained by considering how the electron attachment energy changes in going from the geometry of the anion to that of the neutral. The corresponding potential energy curves are shown in Fig. 1, where straight line cuts through the two respective minima (defined in terms of bond length R and bond angle θ by the respective two points $[R_0, \theta_0]$ and $[R_-, \theta_-]$, see Table 1) have been studied. Clearly, the adiabatic potential curves of CO_2^- and OCS^- do not simply "cross" into the continuum, but bend towards the curves of their associated neutrals, forming barriers before the attachment energies become negative and the anionic states become resonances. In the region of the barrier, the wave function of the anion changes its character from valence to diffuse, and this change strongly influences the properties of the long-lived anion as well as the electron scattering processes from the neutral in the energy region below the anionic minimum [40,43]. For CO_2, this effect is much stronger than for OCS, whereas for CS_2 the curves of the neutral and the anion do not cross in the investigated part of the nuclear coordinate space, since at the employed theoretical level even the vertical electron affinity (VEA) is found to be slightly positive. We find also at the higher CCSD(T)/AUG4 level a positive VEA of 8 meV for CS_2, and thus predict that for a substantial part of the Franck–Condon zone the potential energy surfaces of the anion is below the surface of neutral CS_2. Consequently, for CS_2 the character of the crossing is not expected to be as relevant as for CO_2 or OCS.

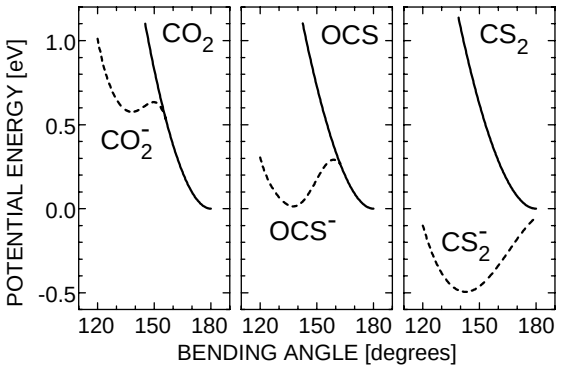

Fig. 1. Cuts through the potential energy surfaces of CO_2, OCS, and CS_2 (full curves) and of their anions (broken curves). Straight line cuts through the equilibrium geometries of the respective neutral/anion pairs have been studied (see text). The energy of the neutrals was computed at the CCSD(T)/AUG3 level, and the curves of the anions have been obtained from the electron affinities computed at the EOM-CCSD/AUG3$^+$ [4s4p2d] level.

3. Properties of $(OCS)_2^-$ anions

While negatively charged carbon dioxide and carbon disulfide clusters have been subject of many studies (see Section 1 and, e.g., references in [22]), the structures and spectrosopic properties of $(OCS)_q^-$ cluster anions have only recently been investigated [44–46]. In particular for the dimer anion several possible structures were discussed and investigated theoretically [44] as well as spectroscopically [45,46]. It was found that $(OCS)_q^-$ cluster anions do possess a far richer photochemistry than the analogous negatively charged CO_2 cluster ions. For example, in photodissociation three types of ionic products were identified following excitation at 395 and 790 nm: $(OCS)_qS_2^-$, $(OCS)_qS^-/(OCS)_{q-1}OCS_2^-$, and $(OCS)_q^-$, and the size distribution in the cluster anion mass spectra exhibited a strong dependence on the photon energy. This behaviour is due to a greater structural flexibility of $(OCS)_q^-$ cluster anions which can, in contrast to $(CO_2)_q^-$ cluster anions, form weak covalent S–S bonds.

$(CO_2)_q^-$ anion clusters show two different types of structures [47–50]. On the one hand, there are clusters with monomer anion cores, that is, the excess electron is localised on one particular CO_2 monomer and the other CO_2 units essentially solvate the CO_2^- anion. We will refer to these species as type-I clusters, and note that the type-I dimer has also been addressed as "electrostatically bound" and as "van der Waals complex." On the other hand, the electron can be localised on an oxalate-like $C_2O_4^-$ anion that possesses a covalent C–C bond. These clusters are referred to as type-II or dimer-anion-core structures. Since $(OCS)_q^-$ cluster anions can in addition form weak covalent S–S and C–S links, there is a wider variety of type-II isomers, e.g., only C–C linked, C–C and S–S linked, etc. [44]. In particular, a C–C and S–S linked dimer forming a four-membered ring was found to be the most stable isomer and to possess low-lying

electronically excited states, a qualitatively new property in comparison with CO_2 cluster anions [44].

In the present context the primary interest is the attachment process at low electron energies, and here we aim at getting a reasonably accurate idea of how much energy is in principle available—or rather needs to be dissipated—after electron attachment and what kind of process can be initiated by a low energy electron. Structures, relative energies, and a C_{2v} constrained cut through the adiabatic PES along the C–C bond breaking coordinate of different anionic species (and neutral/anion pairs), obtained at the second order many body perturbation theory (MP2) level, have been given in reference [44]. We reinvestigated several of these species as well as two possible structures of the neutral OCS dimer at the CCSD(T) level, since higher order correlation effects beyond MP2 are known to be important for the computation of the electron affinity of the OCS monomer as well as for the electron binding properties of the analogous CO_2 clusters.

In the following, we briefly present energies obtained at the CCSD(T)/AUG3 level, employing CCSD(T)/AUG2 geometries and CCSD/AUG2 zero-point energy corrections. At this level of theory the AEA of the OCS monomer is predicted to be −5 meV, very close to the best value discussed in Section 2. We considered two structures of the OCS dimer that are both derived from the well-known C_{2h} symmetrical CO_2 dimer (see, e.g., [51]). Owing to the lower symmetry of the OCS monomer, there are two C_{2h} symmetrical OCS dimer structures, one with the O atoms (Fig. 2, upper right), and one with the S atoms pointing "outward" (Fig. 2, upper left). The energy of the O-outward isomer is slightly lower, and the binding energies of the two $(OCS)_2$ van der Waals clusters are 79 and 68 meV, respectively, in the same order of magnitude as that of the CO_2 dimer. Relative to the lower OCS dimer, the AEA of the $OCS{\cdot}OCS^-$ type-I cluster anion (C_1 symmetry; Fig. 2, lower left) is found to be 0.15 eV, and that of the lowest type-II dimer anion (C_{2v} symmetry [44]; Fig. 2, lower right) is predicted as 0.58 eV.

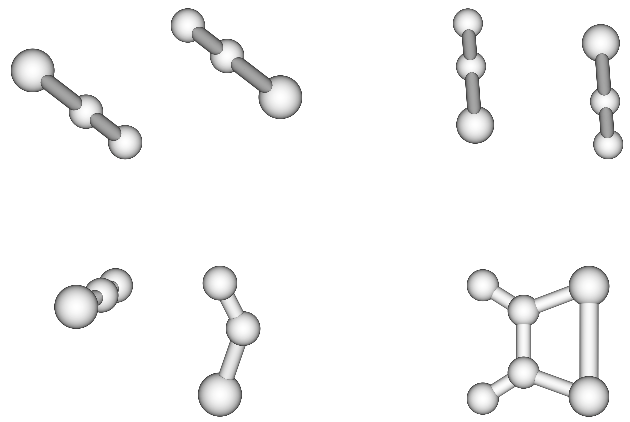

Fig. 2. Geometrical structures of neutral and anionic OCS dimers discussed in the text. The structures have been computed at the CCSD(T)/AUG2 level of theory. Upper left: $(OCS)_2$ S-outward isomer; upper right: $(OCS)_2$ O-outward isomer; lower left: $(OCS)_2^-$ type-I cluster; lower right: $(OCS)_2^-$ type-II cluster.

As far as we can compare these energies with the values given in reference [44] the agreement with the MP2 results is astonishingly good, yet the more recent values (obtained with the B3LYP hybrid functional [46]) clearly overestimate the dimer's electron affinity considerably. All in all, in contrast to CO_2^-, already the OCS^- monomer is at the brink of electronic stability, and the type-I and type-II $(OCS)_2^-$ anions possess substantial electron binding energies.

4. Experimental setup and test measurements

Our experiment is based on the laser photoelectron attachment (LPA) method introduced by Klar et al. [9,52]: energy-variable, monoenergetic electrons are created by laser photoionization of laser-excited atoms in a collimated beam and interact with the target molecules (clusters) of interest in the region where the photoionization process takes place. In the present work, we apply the variant of the LPA method introduced by Weber et al. [12,19,29] (see Fig. 3).

The electrons are produced by two-step laser photoionization of potassium atoms in a collimated beam (collimation 1:400, diameter 1.5 mm) from a doubly differentially pumped metal vapour oven [29,53]. Both hyperfine components of ground state ^{39}K (4s, $F = 1, 2$) atoms are transversely excited to the $^{39}K^*$ ($4p_{3/2}$, $F = 2, 3$) states by the first sidebands $f_1 \pm \Delta f$ of the electro-optically modulated ($\Delta f = 220.35$ MHz) output of a stabilized single mode cw Titanium:Sapphire laser ($\lambda_1 = 766.7$ nm, frequency f_1) (see Fig. 4). Part of the excited state population is transferred to high Rydberg levels (nd, $(n + 2)$s, $n \geq 12$) or photoionized by interaction with the intracavity field of a broadband (40 GHz = 0.16 meV) tunable dye laser (power up to 5 W), operated in the blue spectral region ($\lambda_2 = 472$–424 nm, dye Stilbene 3). The energy of the photoelectrons can be continuously varied over the range 0–200 meV by tuning the wavelength of the ionizing laser ($\lambda_2 < 455$ nm).

Electrons, created in the overlap volume of the potassium atom beam and the laser beams, may attach to molecules and

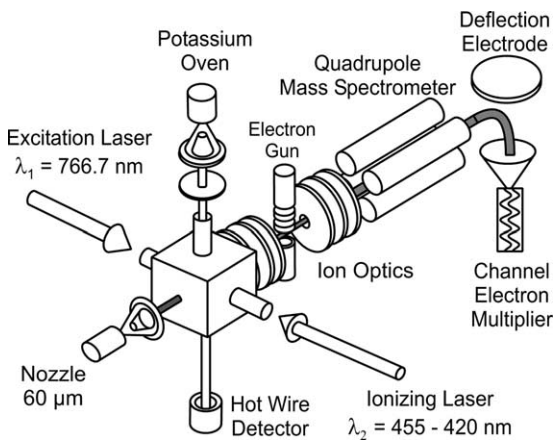

Fig. 3. Schematic view of the setup for the laser photoelectron attachment experiment.

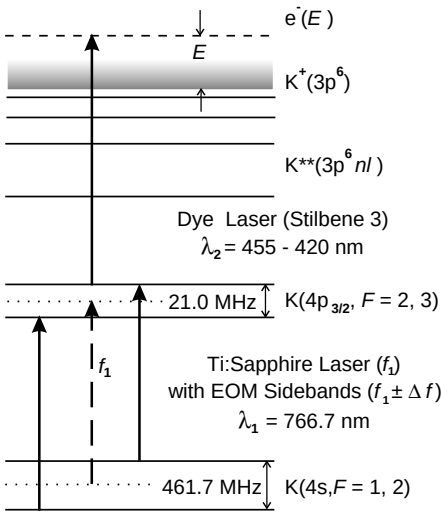

Fig. 4. Excitation scheme of the laser photoelectron source for the LPA experiment.

clusters in a collimated, differentially pumped seeded supersonic beam, propagating in a direction perpendicular to both the potassium and the laser beams. The target beam has a diameter of 3 mm in the reaction region and originates from a nozzle with 60 μm diameter at a nozzle temperature of $T_0 = 300$ K and stagnation pressure of $p_0 = 3$ bar (10% OCS in He, supplied by Praxair GmbH). Anions, generated by electron attachment and drifting out of the essentially field free reaction chamber, are imaged into a quadrupole mass spectrometer ($m/q \leq 2000$u/e) and detected by a differentially pumped off axis channel electron multiplier (background counting rate about 0.02 s^{-1}). The reaction volume is surrounded by a cubic chamber made of oxygen free, high conductivity copper, the inner walls of which are coated with colloidal graphite. By applying bias potentials to each face of the cube, dc stray electric fields are reduced to values $F_S \leq 0.1$ V/m. Magnetic fields are reduced to values below 2 μT by compensation coils located outside the vacuum apparatus. The electron energy resolution is limited by the bandwidth of the ionizing laser ($\Delta E_L \approx 0.16$ meV), residual electric fields ($\Delta E_F \leq 0.3$ meV), the Doppler effect caused by the target velocity ($\Delta E_D \approx 0.07E^{1/2}$, ΔE_D and electron energy E in meV), and space charge effects due to K^+ photoions generated in the reaction volume (depending on the K^+ current) [54]. Simulations and measurements indicate that the space charge broadening amounts to about 0.033 meV/pA (FWHM) for the conditions of the attachment experiment [54]. For the sake of normalization and in situ resolution testing, measurements of SF_6^- formation were frequently carried out, using a seeded supersonic beam of about 0.05% SF_6 in He ($p_0 = 1$ bar, $T_0 = 300$ K). By comparison of the measured anion yield with the known cross section for SF_6^- formation [6,9,55] near 0 eV (convoluted with adjustable resolution functions), the effective electron energy spread at low energies can be inferred. From this comparison and the information gained on the energy broadening due to the photoion space charge [54], we estimate the overall energy spread (FWHM) at low energies to be typically 1–2 meV at electron currents in the range 20–50 pA.

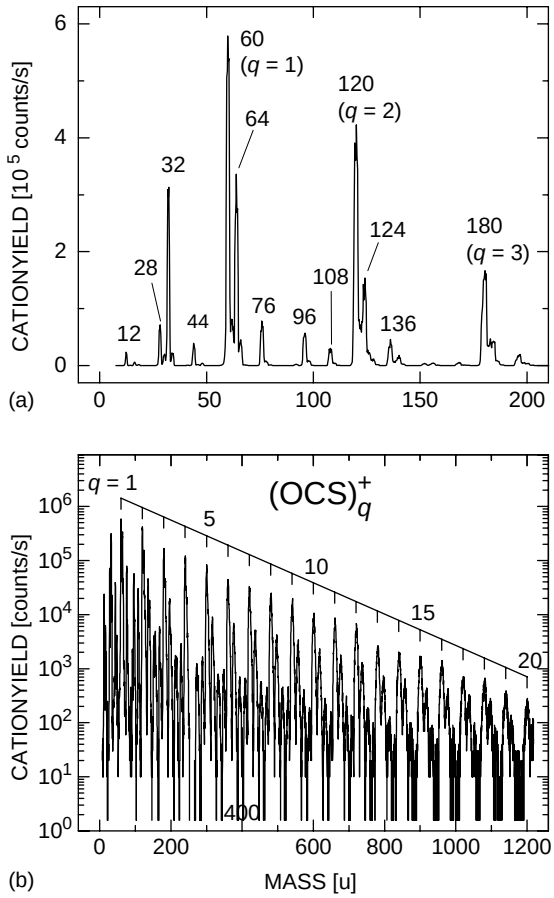

Fig. 5. Mass spectrum of positive ions resulting from 85 eV electron impact of a collimated cluster beam, formed by supersonic expansion of a mixture of 10% OCS in helium carrier gas at 3 bar and 300 K. (a) An enlarged view of the spectrum at low masses ($m/q \geq 10$u/e) with a linear intensity scale; the assignment of the masses is given in Table 2.

The composition of the cluster beam was routinely monitored by measuring the mass spectra of positive ions due to 85 eV electron impact, using an auxiliary, standard electron gun at a current of about 1 μA, placed between the LPA reaction chamber and the entrance hole of the mass spectrometer. The mass spectrum of positive ions is dominated by homogeneous cluster ions $(OCS)_q^+$, as seen in Fig. 5.

Under the experimental conditions relevant for the investigations described in Section 5, the $(OCS)_q^+$ intensities decrease nearly exponentially in the size range of interest (by about three decades from $q = 2$ to $q = 20$). Although the positive ion mass spectrum is not a direct image of the neutral cluster size distribution, the measured positive ion mass spectrum indicates that the size distribution for the neutral clusters $(OCS)_N$ varies smoothly for $N = 2$–20. Fig. 5a shows a detail of the mass spectrum (mass range 10–210 u), and the mass assignment is presented in Table 2. We note that the peaks at 76 and 136 u may be attributed to the

Table 2
Assignment of the positive ion mass peaks, observed at the indicated mass to charge ratios (u/e) in Fig. 5a, to the respective possible species, resulting from 85 eV electron impact of the OCS cluster beam which contains a small CS_2 impurity

Mass	Positive ion fragment
12	C^+
28	CO^+
32	S^+/O_2^+
44	CS^+/CO_2^+
60	OCS^+
64	S_2^+
76	$(OCS)O^+/CS_2^+$
96	S_3^+
108	$(OCS)OS^+$
120	$(OCS)_2^+$
124	$(OCS)S_2^+$
136	$(OCS)_2O^+/(OCS)CS_2^+$
180	$(OCS)_3^+$

combinations $OCS{\cdot}O^+/CS_2^+$ and $(OCS)_2{\cdot}O^+/OCS{\cdot}CS_2^+$, respectively.

Negative ion mass spectra, due to Rydberg electron transfer (RET) involving $K^{**}(nl)$ Rydberg atoms, show homogeneous $(OCS)_q^-$ ($q \geq 2$) cluster anions as dominant species, and, very weakly, OCS^- ions. In Table 3, we quote typical intensities observed for the $(OCS)_q^-$ ($q \geq 1$) anions due to Rydberg electron attachment at high principal quantum numbers n ($n \approx 260$) when the ion optics was optimized for each cluster size separately. In Fig. 6 we compare the $(OCS)_q^-$ ($q \geq 1$) anion intensities due to RET at high n with the intensities of the positive $(OCS)_q^+$ ($q \geq 1$) ions, observed in 85 eV electron impact.

It was found that the q-dependent cluster anion intensity ratios $I_q(n)/I_{q=2}(n)$ ($q = 1$–12) were, to within a factor of two or less, independent of n at principal quantum numbers lower than about $n \approx 50$, while these ratios were found to decrease rather strongly (by factors around 4) with n rising to $n \approx 260$ (Rydberg electron binding energy ≈ 0.2 meV). The latter observation reflects the fact that the rate coefficient for $(OCS)_2^-$ formation is especially high at very low electron energy.

In addition to the homogenous cluster anions, mixed cluster anions of the type $(OCS)_{q-1}CS_2^-$ ($q \geq 1$) (i.e., CS_2^- for $q = 1$) were observed at levels of a few percent. For energetic reasons, they cannot be assigned (as possible for positive ions at the respective masses) to ions of the type $(OCS)_qO^-$ ($q \geq 1$). The observation of these (unexpected) anions $(OCS)_{q-1}CS_2^-$ ($q \geq 1$) is attributed to an impurity of CS_2 molecules in the OCS sample (probably accompanied by a corresponding impurity of CO_2 molecules).

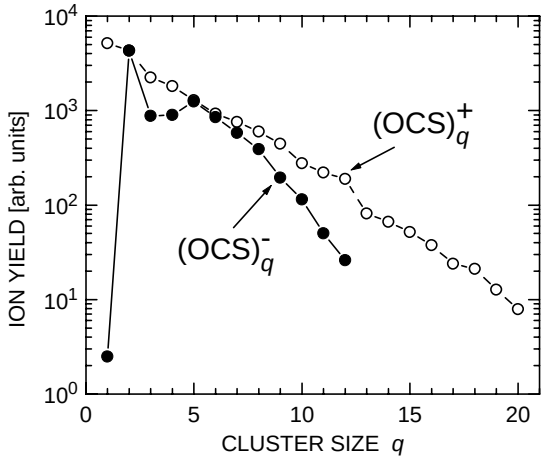

Fig. 6. Intensities of homogeneous positive ions (open circles) and negative ions (full circles, normalized at $q = 2$) due to 85 eV electron impact and threshold electron attachment (Rydberg electron transfer at $n \approx 260$) respectively, involving an OCS cluster beam, formed by an expansion of 10% OCS in helium at 3 bar and 300 K.

5. Experimental results and discussion

In Fig. 7 we present the energy dependent yield for $(OCS)_q^-$ ($q = 1$–12) cluster anions over the energy range $E = 1$–200 meV. These measurements were carried out at an electron current of $I_e = 30$ pA. All the spectra have a common intensity scale (corresponding to the respective cluster anion intensities in Table 3, as observed for RET at high n), and exhibit a distinct zero energy peak, indicative of s-wave attachment. The spectrum observed for the molecular anion OCS^- ($q = 1$) shows a very low counting rate, and only selected energy regions were covered. It exhibits a narrow resonance peaking at about 128 meV (just below the onset for (0 2 0) vibrational excitation at 130 meV), which we interprete as a VFR associated with the $(\nu_1\,\nu_2\,\nu_3) = (0\,2\,0)$ threshold. VFRs are temporary anion states in which the incoming electron is weakly bound in a diffuse orbital to a vibrationally excited molecule or cluster [6,23]. The electron binding may be due entirely to long-range forces (associated with, e.g., a permanent dipole moment and/or the polarizability of the molecule or cluster). The key spectrum is observed for $q = 2$ where the peaks exhibit the narrowest widths (see also Fig. 8, middle trace). Apart from the already mentioned prominent rise towards zero electron energy, it also shows the sharp VFR located at 128 meV, followed by a broader peak (centered at about 117 meV) and structure just around the (0 0 1) onset. Another peak, located at about 59 meV, can be attributed to a VFR associated with the (0 1 0) vibrational onset. The shape

Table 3
Counting rates CR (counts s^{-1}) for the yield of $(OCS)_q^-$ cluster anions ($q = 1$–12) due to Rydberg electron transfer at high principle quantum numbers ($n \approx 260$); ion optics optimized for each cluster anion size q

q	1	2	3	4	5	6	7	8	9	10	11	12
CR	25	43000	8800	9000	12500	8500	5800	3900	1950	1150	500	260

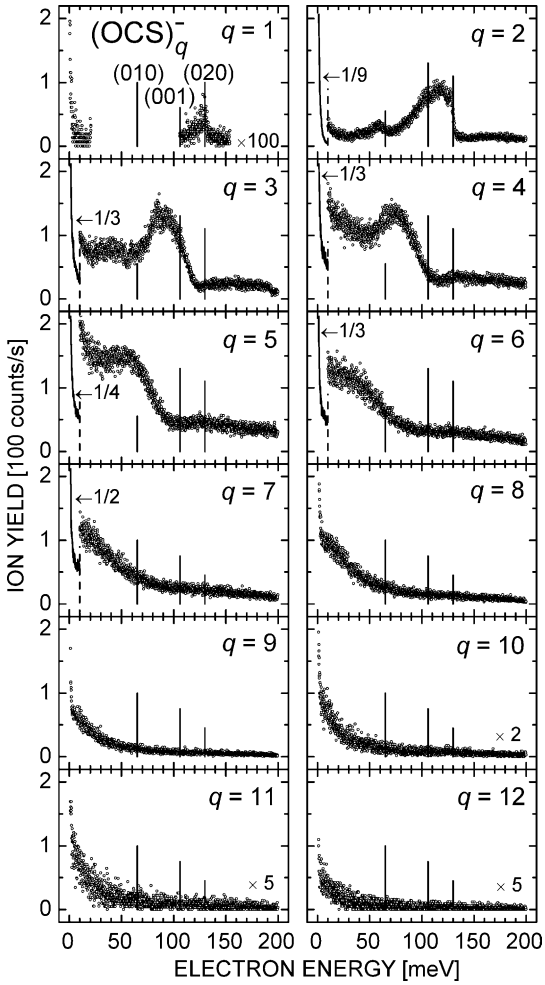

Fig. 7. Low-energy electron attachment spectra for formation of $(OCS)_q^-$ anions ($q = 1$–12) from $(OCS)_N$ clusters ($q \leq N$). The full vertical lines denote the energy positions of the listed vibrational modes in the OCS monomer.

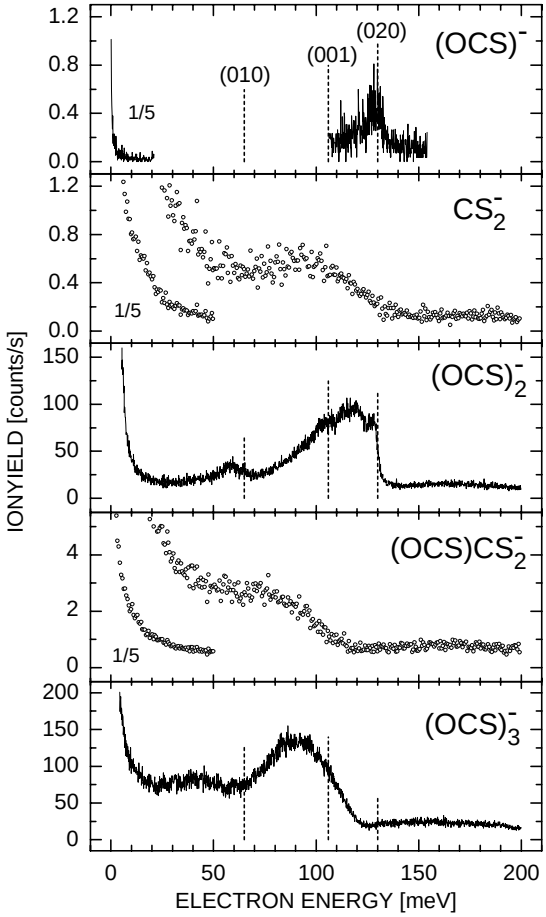

Fig. 8. Attachment spectra for the formation of $(OCS)_q^-$ ($q = 1$–3) and $(OCS)_qCS_2^-$ ($q = 0$, 1) anions. Note that the spectra have different intensity scales. Several data runs were averaged in each case; furthermore, the data points (open circles) for the CS_2^- and $(OCS)CS_2^-$ yields represent five channel averages (point separation 0.6 meV).

of the VFR at 128 meV is similar to the VFR previously observed at about 61 meV in I^- formation via dissociative electron attachment to CH_3I molecules, just below the onset for the $\nu_3 = 1$ C–I stretch vibration [23,29].

The attachment spectra for both $q = 1$ and $q = 2$ exhibit the (0 2 0)-peak essentially at the same energy position, indicating that the yield of the monomer OCS^- is due to primary formation of the dimer anion $(OCS)_2^-$ with subsequent evaporation of a single OCS molecular unit (and not due to attachment of clusters with sizes $q \geq 3$). It is not expected that (longlived) OCS^- anions are formed through *free* electron attachment to OCS monomers because the mechanism which produces metastable ions of, e.g., SF_6^- at near-zero energies, namely resonant electron capture followed by efficient vibrational redistribution into anion states with long autodetachment times [3,6,9–11], will not be operative for a triatomic system. Moreover, capture into the bent OCS^- ground state (which likely is metastable in the light of the potential curves in Fig. 1, see also discussion in [37]) is strongly suppressed by unfavorable Franck–Condon factors. We note that OCS^- formation is only a weak channel in the RET anion mass spectra as well, both at $n = 20$ and at $n \approx 260$. For RET at lower n, OCS^- formation from OCS monomers might have been considered possible via post-attachment stabilization [56] of the OCS^- anion through momentum and energy exchange within the K^+–OCS^- complex, formed in the primary electron transfer process. This type of stabilization has been demonstrated, for instance, in RET to CS_2 molecules at $n \leq 20$ [57–60]. Possibly, the needed geometry change to produce long-lived OCS^- ions is too large as to be efficiently induced by post-attachment interactions in the K^+–OCS^- complex.

In the attachment spectrum for $(OCS)_3^-$ cluster anion formation (see Figs. 7 and 8), the sharp peak in the spectrum for dimer anions, assigned to a VFR associated with the (0 2 0) vibrational onset, is no longer observed. The peak maximum is red-shifted by about 27 meV with respect to the corresponding broad peak in the dimer anion spectrum. At lower energies another weak peak is observed around 40 meV, red-shifted by about 19 meV with respect to the corresponding weak peak in the dimer spectrum.

With rising cluster size ($4 \leq q \leq 7$), the peak structure broadens progressively with onsets shifting by about 10 meV towards lower energy per added monomer unit (Fig. 7). For $q > 7$ no clear peak structure is left in the spectra which are dominated by the rise towards zero energy. The missing of the sharp (0 2 0) resonance for $q > 2$ has an analogy in the findings for electron attachment to $(CH_3I)_q$ clusters [23,29]: the sharp VFR observed at about 61 meV (just below the onset for the C–I stretch vibration $\nu_3 = 1$) for dissociative attachment to methyl iodide monomers (yielding I^- ions) is missing in the attachment spectra for $(CH_3I)_qI^-$ cluster anions, which exhibit only weak, broadened and red-shifted structure for $q = 1$ and practically no structure for $q = 2$. These findings were interpreted by model *R*-matrix calculations [29], which suggest that two mechanisms are responsible for the disappearance of the VFR: a shift of the negative-ion curve due to solvation and interaction with soft-mode vibrations which destroy the resonance and, in addition, smear out the pronounced cusp structure at the $\nu_3 = 1$ threshold observed in dissociative attachment to the monomer [29].

At higher electron energies (between 150 and 200 meV) the attachment spectra for $q = 2$–7 show a counting rate that is clearly higher than zero, in particular for $q = 4$ and $q = 5$. This behaviour may possibly be attributed to the influence of VFR structure associated with the symmetric stretch mode (1 0 0), located at 255.7 meV for the monomer. Measurements extending to higher energies are desirable to confirm this interpretation.

Apart from the homogeneous $(OCS)_q^-$ anions, we have also observed weak anion signals attributed to the species $(OCS)_qCS_2^-$ ($q \geq 0$). Attachment spectra were taken for the anions CS_2^- and (OCS) CS_2^-; they are shown in Fig. 8 and compared with the yield functions for the homogeneous anions $(OCS)_q^-$ ($q = 1$–3). The spectra for CS_2^- and $(OCS)CS_2^-$ exhibit a zero energy peak and broad shoulders with onsets around 130 and 120 meV, respectively, attributed to the influence of VFR structure. These onsets agree with those observed in the spectra for the homogeneous dimer and trimer anions, respectively. Note that the sharp VFR in the dimer anion spectrum (which we interpret to be an attachment characteristic of the neutral dimer cluster) is missing in the spectrum for CS_2^- formation. We propose that the spectra observed for the homogeneous dimer and trimer anions is due to electron attachment to the neutral dimer and trimer cluster, respectively, while the spectra for CS_2^- and $(OCS)CS_2^-$ formation are due to electron attachment to the mixed neutral clusters $(OCS)CS_2$ and $(OCS)_2CS_2$. The fact that the onsets of the VFR structure in the spectra for the $(OCS)_q^-$ ($q = 2$, 3) anions essentially agree with those for the VFR structure in the spectra for the $(OCS)_qCS_2^-$ ($q = 0$, 1) anions indicates that the solvation shift in the respective temporary anions is essentially the same when a CS_2 molecule replaces a OCS monomer. We note that the CS_2^- anion yield does not arise from attachment to pure CS_2 clusters for two reasons: (i) in this experiment, CS_2 molecules are much less abundant than OCS, (ii) the yield for CS_2^- formation from pure CS_2 clusters shows no structure in the respective energy range [22].

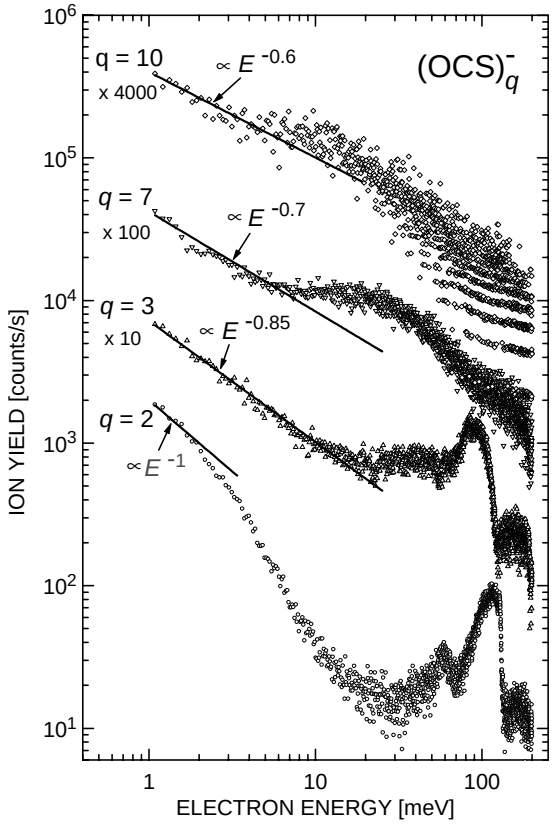

Fig. 9. Double-logarithmic plot of the attachment spectra for $(OCS)_q^-$ ($q = 2$, 3, 7, 10) cluster anion formation. The energy dependence very close to zero energy follows a E^{-X} dependence with X in the range 0.6–1.0, compatible with s-wave capture.

When the $(OCS)_q^-$ attachment spectra of Fig. 7 are plotted on a double-logarithmic scale, additional information on the shapes of the attachment curves at very low energies is revealed. These plots are shown in Fig. 9 for the selected cluster sizes $q = 2$, 3, 7, 10. At very low energies ($E < 5$ meV) the attachment yields exhibit a behaviour proportional to E^{-X}, where the parameter X assumes values between 0.6 and 1.0 as a function of cluster size q. These values of X are given with an uncertainty of ± 0.05. This behaviour of the electron attachment cross section, which rises towards very low energies, suggests that the electron-cluster interaction occurs through s-wave capture [12,19,61,62]. Fig. 9 also clearly reflects the importance of the VFR structure in the $q = 2$ spectrum and the disappearance of the VFR structure towards higher anion size q.

In Fig. 10 we compare cluster attachment spectra for the isovalent series CO_2, OCS, and CS_2 for selected anion sizes q. Formation of CO_2 cluster anions predominantly proceeds through VFRs which act as doorway states towards anion formation by providing time for the nuclear framework to reorganize into non-autodetaching anion states. On the contrary, no VFR structure is observed for CS_2 cluster anion

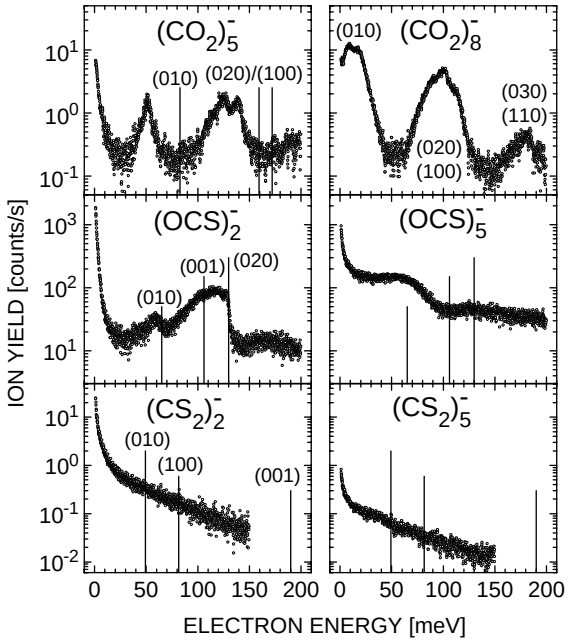

Fig. 10. Comparison of attachment spectra for formation of homogeneous cluster anions $(CO_2)_q^-$ (q = 5, 8), $(OCS)_q^-$ (q = 2, 5), and $(CS_2)_q^-$ (q = 2, 5). VFRs dominate the spectra for $(CO_2)_q^-$ formation, are still prominent (though broader) in the $(OCS)_q^-$ spectra, but absent in the $(CS_2)_q^-$ spectra.

formation while OCS presents an intermediate case. It is of interest to correlate these findings with the electron scattering and binding properties of the respective monomers.

The adiabatic electron affinities rise in steps of about 0.5 eV from CO_2 (≈−0.5 eV) via OCS (≈0 eV) to CS_2 (≈+0.5 eV, see Section 2). The vertical electron affinities for the geometry of the respective linear ground state molecule (i.e. the relevant quantities for a "sudden" attachment process in the spirit of the Franck–Condon principle) rise strongly from −3.8 eV ($^2\Pi_u$ shape resonance) for CO_2 to ≈0 eV for CS_2. Electron scattering from CO_2 at energies below 1 eV is, however, strongly influenced by a virtual state [6,24–26] which evolves into a bound state upon bending (and stretching) of the molecule, as illustrated in Fig. 1. This scenario is reflected in the experimental observation of VFRs in the near-threshold excitation of certain higher-lying Fermi-coupled vibrations in CO_2 involving symmetric stretch and bending [43]. These vibrational resonances owe their existence to the fact that the electron largely resides in a diffuse long-range bound orbit which does not autodetach for a sufficiently bent and stretched nuclear framework. Around the linear geometry the CO_2^- starts to loose the extra electron since it is no longer bound in the adiabatic sense. The near-threshold electron departs only slowly, however, and part of the outgoing wave function is recaptured when the nuclei swing back to the bent geometry again, giving rise to VFRs of varying widths [6]. The VFRs observed in the attachment spectra for the formation of $(CO_2)_q^-$ ($q \geq 4$) cluster anions may well represent the solvation-shifted analogues of the VFRs just discussed for the monomer. The redshifts of the cluster anion resonances (relative to the monomer vibrational level energies) were recovered with a simple model in which the extra electron is bound by a combination of the long-range polarization potential with an attractive potential inside the cluster [21,22]. More recent high level ab initio studies of electron binding to small CO_2 clusters have shown [27] that anion clusters with sizes $q \geq 4$ are stable, but the nature of the experimentally observed VFRs has still to be understood in more detail.

For CS_2 the vertical electron affinity is near 0 eV (see Section 2). Long-lived weakly bound CS_2^- anions are formed in Rydberg electron transfer (RET) to CS_2 molecules at medium principal quantum numbers [57–60]. The rate coefficient for this process shows a broad maximum around $n \approx 18$ [58,60], reminiscent of n dependences observed for the formation of dipole bound anions [63,64]. Dunning's group showed that these CS_2^- anions are subject to field detachment in rather small electric fields of a few kV cm^{-1} [57]. Strong and sharp CS_2^- resonances have been observed in the energy dependence of the total cross section [65] as well as of the angle differential elastic cross section [66] for scattering of free electrons from CS_2 molecules at very low energies (<0.1 eV). The origin of these resonances is still under debate [6]; note that the vibrational spectrum of the valence states of CS_2^- exhibits a very large density of states in this energy range. $(CS_2)_2^-$ anions have been predicted [67] to exist as stable species with adiabatic electron affinities >0.3 eV relative to $CS_2 + CS_2^-$. It is expected that the vertical electron affinity of $(CS_2)_q$ clusters ($q \geq 2$) is also positive and rising with increasing q due to solvation. According to the absence of VFR structure in the attachment spectra for CS_2 clusters the effects of solvation quench vibrational resonance structure, which is so clearly present in the electron scattering cross sections for the CS_2 monomer, in a way similar to the trend observed for methyl iodide molecules and clusters [29].

No high resolution electron scattering experiments on OCS monomers at very low energies have been reported yet to our knowledge, but it may be expected that VFR structure will be present at energies lower than for CO_2. VFR structure is clearly observed in the attachment spectra for $(OCS)_q^-$ cluster anions with small size q (see Fig. 7), but gets lost for larger sizes due to the effects of solvation. The high yield for dimer anions at near-zero electron energies (including RET at high n) and the sharp (0 2 0) VFR in the attachment spectrum of the dimer anion are especially remarkable and point to the existence of a "real" zero energy resonance, i.e., a strong diffuse electron capture state of the neutral precursor cluster (which we propose to be the OCS dimer). In the attachment spectra for $(CO_2)_q^-$ cluster formation, VFR structure persists up to the largest anion sizes studied (q = 34). The corresponding redshifts for the VFRs

have increased to values around 200 meV, and it would be of interest to explore the VFRs in CO_2 clusters up to even larger sizes q. In summary, the tendencies observed in Fig. 10 can be related nicely to the evolution of the properties of the respective neutral and anionic monomers, most importantly to the substantial rise in both the adiabatic and vertical electron affinity from CO_2 to CS_2.

6. Conclusions and perspectives

Using the laser photoelectron attachment method, we have studied the formation of $(OCS)_q^-$ (q = 1–12) cluster anions in low-energy electron attachment (E = 1–200 meV) to molecular clusters of carbonyl sulfide OCS at high resolution (energy width 1–2 meV). The attachment spectra (i.e., the energy dependences of cluster anion formation) are characterized by a strong rise towards zero energy attributed to s-wave attachment as well as—below the onsets of the (0 1 0), (0 0 1), and (0 2 0) vibrational modes of the OCS molecule—by VFRs whose importance decreases towards larger cluster sizes q. Formation of the $(OCS)_2^-$ anion is especially enhanced at near-zero electron energies; moreover, the attachment spectrum exhibits a sharp VFR resonance just below the onset for excitation of the (0 2 0) mode in the OCS molecule. The electron attachment behaviour of OCS clusters is intermediate between that of CO_2 clusters (which is dominated by VFRs) and that of CS_2 (which exhibits a strong zero energy peak, but no VFRs). This finding is correlated with the properties of the respective molecular neutrals and anions which have been studied using very high level ab initio methods. The role of VFRs as doorway states into valence-type anion states is discussed.

So far, strong VFR structure has been observed in the attachment spectra for clusters composed of molecules whose vertical electron affinity is negative (N_2O, CO_2, and OCS). In the future it would be of interest to search for VFR structure in the attachment spectra of molecular clusters which form stable anions involving delocalized electrons and nuclear geometries close to those of the neutral clusters (e.g., dipole-bound anions such as $(H_2O)_2^-$ [68] or $(CH_3CN)_3^-$ [63]). Other systems of interest include molecules and clusters which exhibit both valence-type and diffuse, long-range bound anions [63,64]. VFR structure associated with, e.g., dipole bound states may be “quenched” by coupling of the dipole bound state with the valence-type anion states, as discussed, e.g. for nitromethane [63,64,69].

Acknowledgements

This work has been supported by the Deutsche Forschungsgemeinschaft through Forschergruppe FOR 307 (*Niederenergetische Elektronenstreuprozesse*). We gratefully acknowledge experimental support by E. Leber and A.J. Yencha at the early stages of this work. We thank I.I. Fabrikant, M. Allan, R.N. Compton, W.C. Lineberger, T.M. Miller and J.M. Weber for helpful discussions.

References

[1] G.J. Schulz, Rev. Mod. Phys. 45 (1973) 423.
[2] H.S.W. Massey, Negative Ions, 3rd ed., Cambridge University Press, Cambridge, 1976.
[3] L.G. Christophorou (Ed.), Electron–Molecule Interactions and their Applications, vols. 1 and 2, Academic Press, New York, 1984.
[4] I. Shimamura, K. Takayanagi (Eds.), Electron–Molecule Collisions, Plenum Press, New York, 1984.
[5] M.J. Brunger, S.J. Buckman, Phys. Rep. 357 (2002) 215.
[6] H. Hotop, M.-W. Ruf, M. Allan, I.I. Fabrikant, Adv. At. Mol. Opt. Phys. 49 (2003) 85.
[7] T.D. Märk, Int. J. Mass Spectrom. Ion Process. 107 (1991) 143.
[8] E. Illenberger, in: C.-Y. Ng (Ed.), Photoionization and Photodetachment, Part II, Adv. Ser. Phys. Chem. vol. 10B, World Scientific, Singapore, 2000, Chapter 10, p. 1063.
[9] D. Klar, M.-W. Ruf, H. Hotop, Aust. J. Phys. 45 (1992) 263.
[10] L.G. Christophorou, J.K. Olthoff, J. Phys. Chem. Ref. Data 29 (2000) 267.
[11] L. Suess, R. Parthasarathy, F.B. Dunning, J. Chem. Phys. 117 (2002) 11222.
[12] J.M. Weber, E. Leber, M.-W. Ruf, H. Hotop, Eur. Phys. J. D 7 (1999) 587.
[13] A. Stamatovic, in: H.B. Gilbody, W.R. Newell, F.H. Read, A.C.H. Smith (Eds.), Electronic and Atomic Collisions, Elsevier Science, Amsterdam, 1988, p. 729.
[14] E. Illenberger, Chem. Rev. 92 (1992) 1589.
[15] C.E. Klots, R.N. Compton, J. Chem. Phys. 69 (1978) 1636.
[16] A. Stamatovic, K. Leiter, W. Ritter, K. Stephan, T.D. Märk, J. Chem. Phys. 83 (1985) 2942.
[17] M. Knapp, O. Echt, D. Kreisle, T.D. Märk, E. Recknagel, in: P. Jena, B.K. Rao, S.N. Kanna (Eds.), Physics and Chemistry of Small Clusters, Plenum, New York, 1987, p. 693.
[18] M. Knapp, O. Echt, D. Kreisle, E. Recknagel, J. Phys. Chem. 91 (1987) 2601.
[19] J.M. Weber, E. Leber, M.-W. Ruf, H. Hotop, Phys. Rev. Lett. 82 (1999) 516.
[20] E. Leber, S. Barsotti, J. Bömmels, J.M. Weber, I.I. Fabrikant, M.-W. Ruf, H. Hotop, Chem. Phys. Lett. 325 (2000) 345.
[21] E. Leber, S. Barsotti, I.I. Fabrikant, J.M. Weber, M.-W. Ruf, H. Hotop, Eur. Phys. J. D 12 (2000) 125.
[22] S. Barsotti, E. Leber, M.-W. Ruf, H. Hotop, Int. J. Mass Spectrom. 220 (2002) 313.
[23] A. Schramm, I.I. Fabrikant, J.M. Weber, E. Leber, M.-W. Ruf, H. Hotop, J. Phys. B32 (1999) 2153.
[24] S. Mazevet, M.A. Morrison, L.A. Morgan, R.K. Nesbet, Phys. Rev. A 64 (2001) 040701.
[25] D. Field, N.C. Jones, S.L. Lunt, J.-P. Ziesel, Phys. Rev. A64 (2001) 022708.
[26] M. Allan, Phys. Rev. Lett. 87 (2001) 033201.
[27] T. Sommerfeld, T. Posset, J. Chem. Phys. 119 (2003) 7714.
[28] G.L. Gutsev, R.J. Bartlett, R.N. Compton, J. Chem. Phys. 108 (1998) 6756.
[29] J.M. Weber, I.I. Fabrikant, E. Leber, M.-W. Ruf, H. Hotop, Eur. Phys. J. D 11 (2000) 247.
[30] T. Kondow, K. Mitsuke, J. Chem. Phys. 83 (1985) 212.
[31] J.-P. Ziesel, G.J. Schulz, J. Milhaud, J. Chem. Phys. 62 (1975) 1936.
[32] I. Iga, M.V.V.S. Rao, S.K. Srivastava, J.C. Nogueira, Int. J. Mass Spectrom. Ion Process. 155 (1996) 99.
[33] D.R. Lide (Ed.), CRC Handbook of Chemistry and Physics, 76th ed., Chemical Rubber Company, Boca Raton, FL, 1995.

[34] T. Shimanouchi, Tables of Molecular Vibrational Frequencies, vol. I, NSRDS-NBS 39, 1972.
[35] R.N. Compton, P.W. Reinhardt, C.D. Cooper, J. Chem. Phys. 63 (1975) 3821.
[36] E.C.M. Chen, W.E. Wentworth, J. Phys. Chem. 87 (1983) 45.
[37] E. Surber, S.P. Ananthavel, A. Sanov, J. Chem. Phys. 116 (2002) 1920.
[38] D.E. Woon, T.H. Dunning, J. Chem. Phys. 98 (1993) 1358.
[39] R.A. Kendall, T.H. Dunning, R.J. Harrison, J. Chem. Phys. 96 (1992) 6796.
[40] T. Sommerfeld, J. Phys. B 36 (2003) L127.
[41] M. Nooijen, R.J. Bartlett, J. Chem. Phys. 102 (1995) 3629.
[42] Computer Code ACESII, Quantum Theory Project, University of Florida, 1998.
[43] M. Allan, J. Phys. B35 (2002) L387.
[44] A. Sanov, S. Nandi, K.D. Jordan, W.C. Lineberger, J. Chem. Phys. 109 (1998) 1264.
[45] E. Surber, A. Sanov, Phys. Rev. Lett. 90 (2003) 093001.
[46] E. Surber, A. Sanov, J. Chem. Phys. 118 (2003) 9192.
[47] S.H. Fleischman, K.D. Jordan, J. Phys. Chem. 91 (1987) 1300.
[48] M.J. DeLuca, B. Niu, M.A. Johnson, J. Chem. Phys. 88 (1988) 5857.
[49] T. Tsukuda, M.A. Johnson, T. Nagata, Chem. Phys. Lett. 268 (1997) 429.
[50] M. Saeki, T. Tsukuda, T. Nagata, Chem. Phys. Lett. 340 (2001) 376.
[51] H. Chen, J.C. Light, J. Chem. Phys. 112 (2000) 5070.
[52] D. Klar, M.-W. Ruf, H. Hotop, Meas. Sci. Technol. 5 (1994) 1248.
[53] I.D. Petrov, V.L. Sukhorukov, E. Leber, H. Hotop, Eur. Phys. J. D 10 (2000) 53.
[54] J. Bömmels, E. Leber, A. Gopalan, J.M. Weber, S. Barsotti, M.-W. Ruf, H. Hotop, Rev. Sci. Instrum. 72 (2001) 4098.
[55] A. Schramm, J.M. Weber, J. Kreil, D. Klar, M.-W. Ruf, H. Hotop, Phys. Rev. Lett. 81 (1998) 778.
[56] F.B. Dunning, J. Phys. B 28 (1995) 1645.
[57] A. Kalamarides, C.W. Walter, K.A. Smith, F.B. Dunning, J. Chem. Phys. 89 (1988) 7226.
[58] K. Harth, M.-W. Ruf, H. Hotop, Z. Phys. D 14 (1989) 149.
[59] H.S. Carman Jr, C.E. Klots, R.N. Compton, J. Chem. Phys. 92 (1990) 5751.
[60] C. Desfrancois, N. Khelifa, J.P. Schermann, T. Kraft, M.-W. Ruf, H. Hotop, Z. Phys. D 27 (1993) 365.
[61] I.I. Fabrikant, H. Hotop, Phys. Rev A 63 (2001) 022706.
[62] D. Klar, M.-W. Ruf, I.I. Fabrikant, H. Hotop, J. Phys. B 34 (2001) 3855.
[63] C. Desfrancois, H. Abdoul-Carime, J.P. Schermann, Int. J. Mod. Phys. B 10 (1996) 1339.
[64] R.N. Compton, N.I. Hammer, Advances in Gas-Phase Ion Chemistry, vol. 4, Elsevier, p. 257.
[65] N.C. Jones, D. Field, J.-P. Ziesel, T.A. Field, Phys. Rev. Lett. 89 (2002) 093201.
[66] M. Allan, J. Phys. B 36 (2003) 2489.
[67] A. Sanov, W.C. Lineberger, K.D. Jordan, J. Phys. Chem. A 102 (1998) 2509.
[68] J.V. Coe, G.H. Lee, J.G. Eaton, S.T. Arnold, H.W. Sarkas, K.H. Bowen, C. Ludewigt, H. Haberland, D.R. Worsnop, J. Chem. Phys. 92 (1990) 3980.
[69] T. Sommerfeld, Phys. Chem. Chem. Phys. 4 (2002) 2511.